Available online at www.sciencedirect.com

ScienceDirect

Current Opinion in Electrochemistry

Review Article

Understanding the nanoscale interactions of surface plasmon-mediated semiconductor surfaces with water and light for renewable energy harvesting and conversion

Shanlin Pan, Md Ashaduzzaman, Xiao Li and Eric Wornyo

Abstract

Photocatalysts integrated with surface plasmon metals serve as an interesting platform for fully understanding how energy harvesting and storage are managed through physical and chemical enhancement processes. Nanoelectrode with a single plasmon metal nanoparticle (NP) provides unique features capable of resolving complex enhancement processes which otherwise cannot be achievable through conventional ensemble averaging methods. Preliminary theoretical results are presented here to illustrate both electrochemical and optical field enhancement characteristics of a single NP when interacting with a semiconductor surface. Potential methodologies to construct single plasmon nanoelectrodes and challenges are discussed in this opinion.

Addresses

Department of Chemistry and Biochemistry, The University of Alabama, Tuscaloosa, AL 35487, United States

Corresponding author: Pan, Shanlin (span1@ua.edu)

Current Opinion in Electrochemistry 2023, **37**:101174

This review comes from a themed issue on **Physical and Nanoelectrochemistry**

Edited by **Jeffrey E. Dick**

For a complete overview see the Issue and the Editorial

Available online 5 November 2022

https://doi.org/10.1016/j.coelec.2022.101174

Keywords

Surface plasmon resonance, Plasmonic metals, Photocatalyst, Solar water splitting, Nanoelectrode, Scanning electrochemical microscopy, Multiphysics modeling, Photoelectrochemical reaction.

Surface-enhanced photoelectrochemical (PEC) systems and challenges

Localized surface plasmon resonance (LSPR) of noble metal

Ultrathin metal films and nanostructured noble metals such as Au and Ag NPs [1–4] exhibit interesting optical properties under light illumination when their conduction electrons near the metal surface are in collective oscillating motion under light illumination. The resonance of these surface charges induced by light waves refers to surface plasmon resonance (SPR) which usually shows both light absorption and scattering characteristics evidenced by one or a few distinct plasmonic peaks in their extinction spectra. A strong electromagnetic (EM) field can be created near the surface of the plasmon active metal due to the charge displacement, and such EM field is localized for nanostructured metals such as spherical particles being referred to as localized surface plasmon resonance (LSPR).

PEC energy storage via LSPR enhancement

There is a global interest in harvesting and storing renewable energy from renewable sources such as solar energy. LSPR has been applied to enhance the power efficiencies of a solar cell and PEC hydrogen generation at the surface of a semiconductor. [5–9] Figure 1a illustrates how solar energy input is managed through charge separation and transport and storage into chemicals through redox reactions when a plasmon metal particle is integrated onto a semiconductor surface. The power efficiency of the photocatalytic reactions (e.g., $R - ne^- \rightarrow O$) is expected to be highly dependent on 1) spectroscopy overlapping and surface chemistry of both semiconductor photoelectrode and plasmonic nanoparticle, 2) potential catalytic characteristics of plasmonic nanoparticle and the semiconductor to enhance reaction rates, and 3) energy level alignment of all components of the system for efficient light absorption, charge separation and transport (Figure 1b and c). Regarding LSPR-enhanced PEC systems with n-type photoanode-enabled water oxidation, the enhanced PEC activities by plasmonic nanostructures for oxygen evolution reaction are primarily through four major mechanisms [10]. The first mechanism involves direct electron transfer from plasmonic metallic NPs to the semiconductor when a semiconductor is sensitized with a plasmonic structure (Figure 1c) [11,12]. For example, numerous recent studies have shown that a visible light PEC response can be observed due to hot electron injection for thin-film electrodes made of TiO_2 modified with Au and Ag NPs [13–18]. A drawback of such structures is that electron injection from the semiconductor to the metallic NPs will take place due to

Figure 1

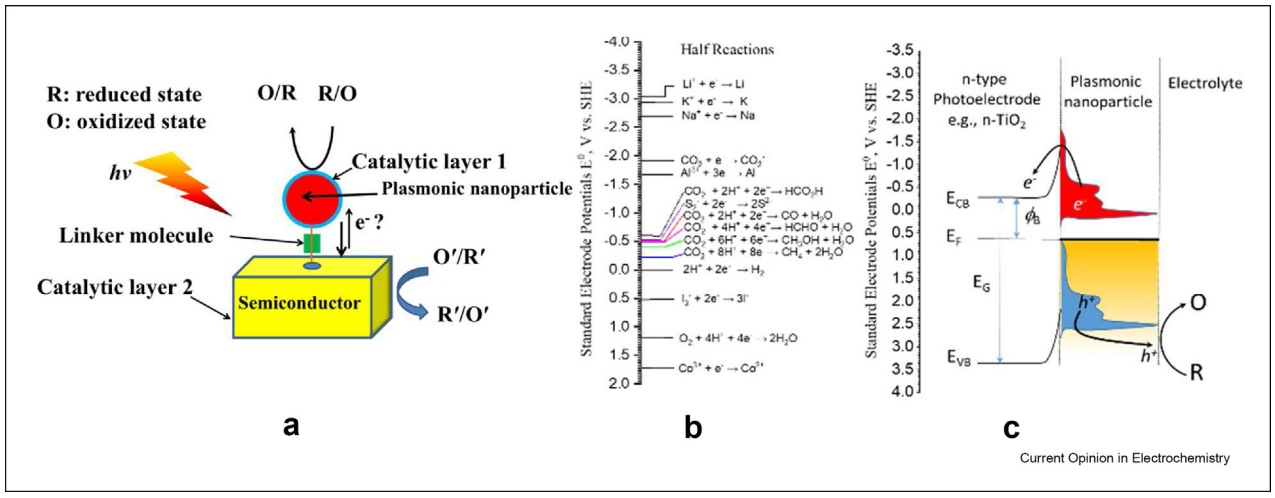

(a) Schematic of catalytic and surface plasmon-mediated semiconductor system for enhanced solar energy harvesting and conversion by optimizing the spectrum overlapping and interfaces, (b) example half reactions and their redox potentials relevant to water splitting and CO_2 reduction and other energy storage systems, and (c) schematic of energy diagram and charge separation of plasmonic nanoparticle-modified n-type photoanode for photocatalytic conversion of R to O.

Fermi level equilibration occurring upon the absorption of light by semiconductor to decrease the plasmon effect [19]. The second mechanism involves the interaction of the semiconductor with localized field enhancement of LSPR to enhance the light absorption cross-section of the semiconductor, thereby increasing its excited state population for improved PEC activities. The third mechanism is based on efficient scattering mediated by SPR (far-field effect), which leads to longer optical path lengths for photons in a semiconductor film to increase the population of excited states. Lastly, local heating thermal upon light absorption of the plasmonic structure may enhance the photoelectrochemical reaction rates [20,21]. The second and third mechanisms are observed in the embedded configuration, where the plasmonic NPs are embedded in the semiconductor material either by conformal coating or by complete coverage [22–24]. Some reports show a decrease in the PEC performance under certain modification conditions with plasmonic metal [25,26]. Because of the inconsistencies in the literature related to plasmon effects on PEC systems [27], further experimental configuration design and theoretical understanding of the plasmon-semiconductor coupling mechanism are needed to improve the enhancement effect by SPR for solar water splitting. There are very limited experimental and theoretical studies in the literature providing direct evidence that can support the plasmonic effect on PEC responses of a photoelectrode because of the use of bulk ensemble averaging PEC measurement methods. PEC studies of single plasmonic NPs are yet to be done to directly compare with theoretical predictions.

Theoretical understanding of single NP LSPR-enhanced PEC and redox activities at a plasmonic nanoelectrode

To resolve the confusion in most experimental reports on plasmon metal-PEC studies, there has to be a well-defined plasmon-semiconductor platform to clarify all factors contributing to the PEC performance. This can be at least addressed theoretically by simplifying the experiment with a model configuration, such as a nanometer-sized tip loaded with plasmonic NP above a photocatalytic surface, to minimize the interference and coupling to/from other plasmonic particles. We can hypothesize that the PEC current enhancement factor (EF) of a bare semiconductor near a surface of single plasmon NPs is given by $EF = \frac{i_p}{i_0} = \left|\frac{E(\lambda)_{ex}}{E(\lambda)^0_{ex}}\right|^2 \eta_{cond.}\eta_{cat.}\eta_{he}$, where i_p is the PEC current in the presence of plasmonic NPs, i_0 is the PEC current of a semiconductor electrode without Au NPs electrode, $\eta_{cond.}$ is the enhancement factor of charge collection through a photoelectrode by the plasmon NPs because of its improved conductivity and collection efficiency, $\eta_{cat.}$ is the catalytic activity enhancement factor derived from the enhanced kinetics when oxygen evolution reaction occurs at the surface of the plasmonic NPs. η_{he} is the enhancement factor of PEC current directly from hot electron injection from plasmon NPs to semiconductors. The first term of the above equation is the integrated spatial distribution of the local field enhancement factor to light absorption cross-section $\left|\frac{E(\lambda)_{ex}}{E(\lambda)^0_{ex}}\right|^2$ under sunlight

illumination. EF is expected to be highly sensitive to photoexcitation direction and polarization angle of the incident light. All enhancement factors in the above equation can be quantified with single NPs electrochemistry and theoretical modeling.

Theoretical modeling can be very complex as it needs to deal with both its electrochemical and optical responses to redox reactions to predict tip current response to the flux of redox molecules in solution or the redox species such as molecular oxygen produced from the photocatalytic substrate. For example, let's start with electrochemical modeling with robust redox model mediators (e.g., $IrCl_6^{2-}$ and ferrocene methanol) which have predictable reaction kinetics and rate constant to calculate the current of a plasmonic NP held by an insulated tip and the spatial distribution of the local redox concentration. Assuming the shape, size, and spatial location of the single plasmonic NP can be precisely determined, one can use the single-particle electrode to approach a PEC semiconductor surface for obtaining more accurate and precise information desired by most experimental efforts in the field [28]. The tip current of the insulated tip holding this plasmonic NP is expected to be sensitive to not only particle size but also the distance to the substrate for the paired NPs system as shown in our calculated results in Figure 2 (previously unpublished results). Local redox concentration profiles and current response at a nanoelectrode with arbitrary shape and size can be calculated to compare with experimental results. An enhanced current response is anticipated from the single plasmonic NP electrode when the tip-to-substrate distance decreases. To generate an improved understanding of the light

Figure 2

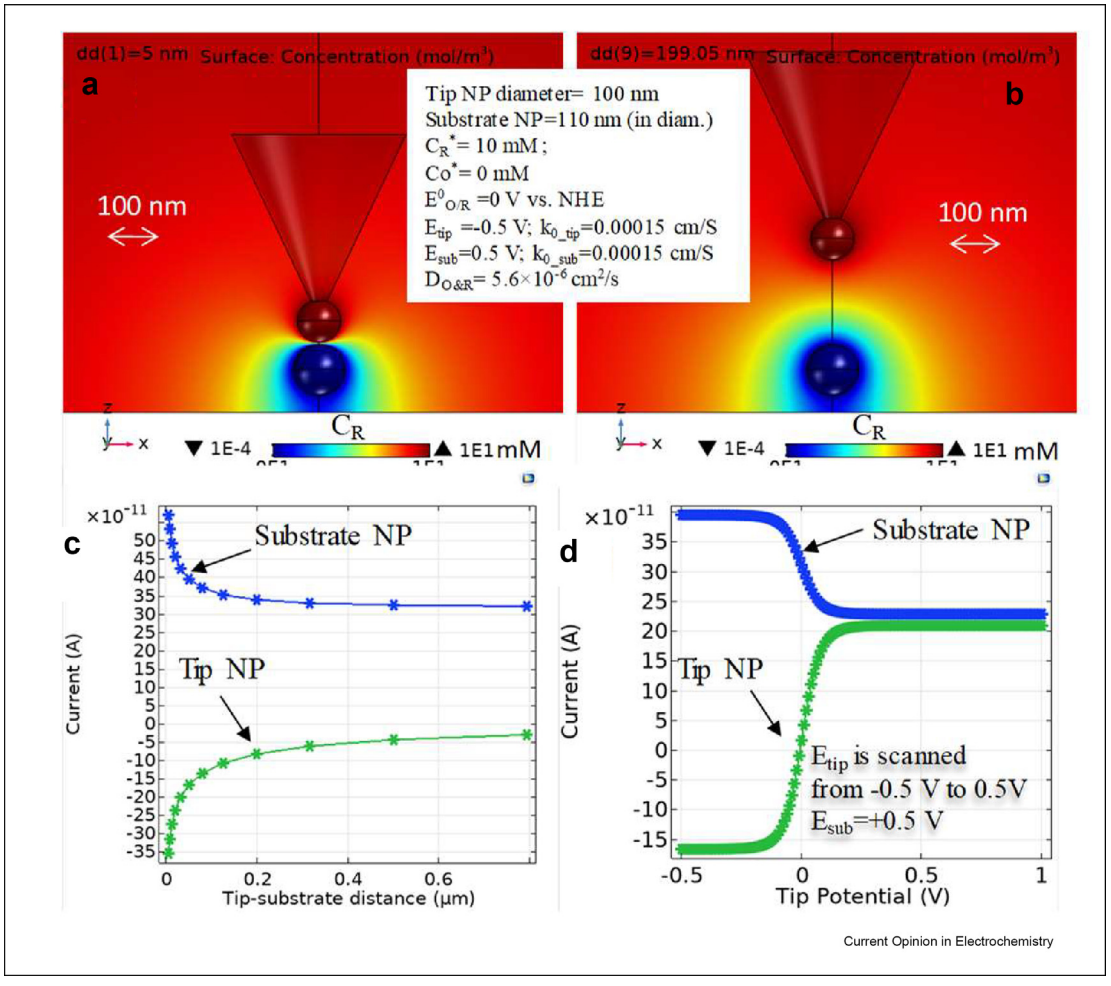

Calculated concentration profile of reduced species (R) at a 100 nm (in diam.) NP when positioned 50 nm (A) and 199 nm (B) away from another 100 nm (in diam.) NP substrate when initial R is oxidized to O via half reaction of R - e^- → O with boundary condition settings shown in the inset. Corresponding approaching curves (C) of tip and substrate NPs when E_{tip} is –0.5 V and E_{sub} is 0.5 V, and linear scanning voltammetry (D) of tip and substrate NPs when tip potential is scanned to reduce O, which is produced from the substrate NP at 0.5 V.

scattering responses and their contribution to the light absorption of a PEC electrode by local field enhancement, for example, a single Au NP held by an insulated tip was used in our preliminary work to model its light scattering properties and the plasmon coupling effects of the embedded plasmonic Au NPs in a semiconductor as shown in Figure 3 (previously unpublished results). As illustrated in Figure 3a, the simulation configuration includes 1) an Au NP coated with a photocatalyst hematite thin film with a known dielectric constant in the visible light region, and 2) a single Au NP held by a sharp dielectric-coated (e.g., polymer or glass) tip. The calculation was done by varying both NP-substrate distance (Figure 3 b & c) and excitation wavelength (Figure 3 d) in radial polarization mode to illustrate how the plasmon coupling along with the vertical axis affects the PEC performance of a hematite interlayer between the two NPs. Changes in scattering intensity upon changing the local refraction index of other redox species can be modeled depending on the electrochemical and optical modeling capability as demonstrated in Figures 2 and 3. Our preliminary calculation results in Figure 3 indicate that the $|E|/|E^0|$ of single plasmonic NPs at 532 nm is greatly enhanced when it is < 100 nm close to other hematite-coated NPs. Details of the modeling are available in the Supplementary Material. A much longer redox coupling distance than 100 nm is expected in Figure 2c, strongly suggesting that we can probe the redox activity of a hematite-modified plasmon NP in either feedback mode or substrate-generation-tip-collection (SG-TC) mode using a single plasmonic NP held by an insulated tip to understand the surface plasmon coupling effects on bare and plasmon-engineered photoelectrode surfaces.

Figure 3

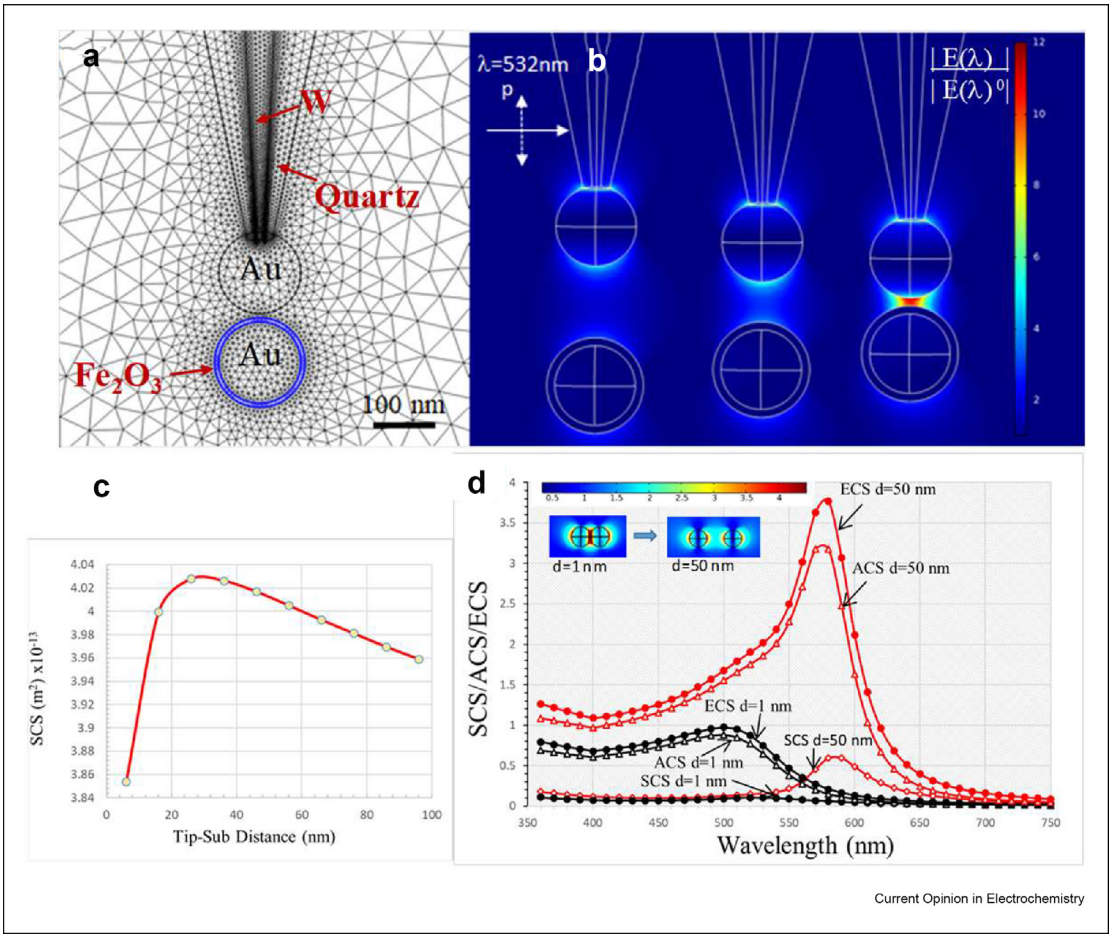

a: Meshed input geometry of a 100 nm (in diam.) Au NP tip loaded onto a quartz glass insulated W tip when position near a 100 nm (in diam.) Au NP coated with a 5 nm hematite thin film; B: Calculated local electric field intensity $|E|/|E^0|$ of the paired Au NPs as shown in A when their distance is 100, 50, and 5 nm from left to right at 532 nm excitation with linearly polarized direction along the vertical axis as shown in figure b; c illustrates the tip-substrate NPs distance dependence of light scattering cross-section of the electrode geometry shown in Figure b; d shows the calculated light scattering (SCS), absorption (ACS), and extinction (ECS) cross-sections dependence on excitation wavelength of a paired Au NPs. Corresponding local field intensity at 532 nm is shown in the inset of panel d.

Current status of single NP electrode-enabled electrochemistry and challenges

There is no experimental report on a single plasmonic NP interacting with a PEC-active surface under electrochemical operation conditions for water splitting. The key component of this desired experimental design is the single plasmonic active nanoelectrode as shown in Figure 3a. Our group recently presented a single plasmon NP electrode with an electrodeposited single Au NP on an insulated sharp W electrode (Figure 4) [29]. The size of Au NP was tuned by adjusting the Au electrodeposition conditions (e.g., electrode potential amplitude and amount of deposition charge). Other conductive nanoelectrode fabrication methods have been reported in the literature that can potentially be improved to benefit the plasmon metal-integrated PEC studies. These studies were initially intended to apply nanoelectrodes for SECM [30,31], Atomic Force Microscopy (AFM) [32], and Scanning Tunneling Microscopy (STM) [33] analysis. Fabrication of nanoelectrode with well-defined geometry and high reproducibility is very challenging due to its delicacy, while it requires reliable insulation (i.e., plasmonic NP held by an insulated tip electrode) to carry out experiments in an in-situ environment. One can make such an insulated nanotip by sharpening a micrometer dimension metal wire to a nanometer tip by chemical etching or by laser-assisted pulling. The sharpened wire is then insulated by polymer or glass either by using chemical vapor deposition (CVD), polymer electrodeposition, or inserting the wire into a glass capillary tube to form a nanoelectrode. Laser-assisted pipette pulling system can be also used to make a sharp metal tip by pulling both a micrometer-sized wire and the quartz/borosilicate capillary simultaneously, while the metal wire is inserted into the capillary before the pulling process. Then, a controlled mechanical polishing or focused ion beam (FIB) treatment is employed to excavate the apex of the nanoelectrode [34,35]. Another popular technique for nanoelectrode fabrication is the electrodeposition of desired metals at the orifice of a prepared nanopipette [36,37]. Additionally, conductive nanoelectrodes with surface insulation can be efficiently produced by pulling a sharp pipette and growing an inner layer of conductive carbon by using either chemical vapor deposition (CVD) [38] or pyrolysis of methane or butane [39] followed by metal NP electrodeposition or surface immobilization. However, making carbon conductive nanoelectrodes with a well-defined geometry is still challenging and time-consuming. Mechanical polishing is typically used to expose a conductive carbon layer during which nanoelectrode can be damaged, delicate handling is thus required. Overall, these are very promising methods that can construct the desired plasmonic tip configuration in Figure 3a.

Once a single plasmonic nanoparticle electrode with a well-defined shape and size is formed based on the strategy outlined above, it will be used as a tip of a conventional scanning probe microscopy under PEC operation conditions. Detailed analysis of the tip current and how it depends on tip-substrate distance and light illumination polarization conditions over a semiconductor surface will provide accurate analysis of each component's contribution to the overall plasmonic enhancement factor, $EF = \frac{i_p}{i_0} = \left|\frac{E(\lambda)_{ex}}{E(\lambda)^0_{ex}}\right|^2 \eta_{cond}.\eta_{cat}.\eta_{he}$, of a surface plasmon-enabled photoelectrochemical system.

Summary

In conclusion, there is a great opportunity to address the global energy challenges by developing efficient PEC systems for renewable energy harvesting and storage,

Figure 4

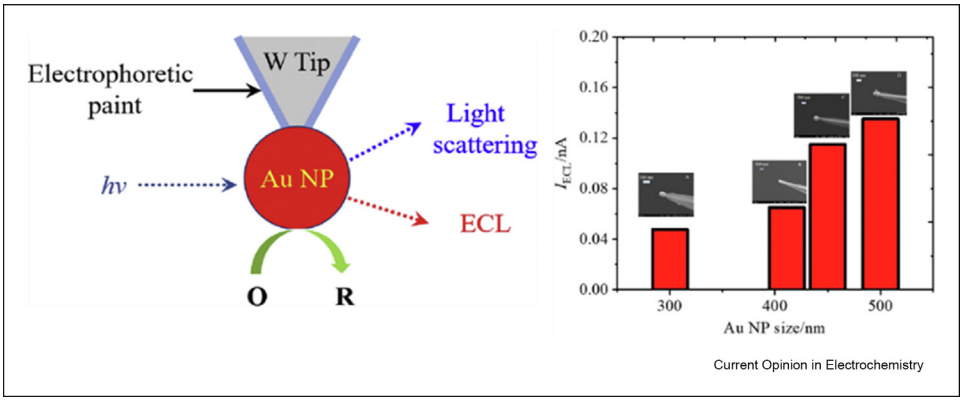

Schematic for single nanoelectrode attached with single Au NP via electrodeposition onto an insulated W nanoelectrode for in-situ spectroelectrochemistry studies. Right: Electrogenerated Chemiluminescence (ECL) intensity of 5.0 mM Ru $(bpy)_3^{2+}$ in 0.1 M PBS (pH 7.4) with 100.0 mM tripropyl amine (TPrA) from four different single Au NPs. *Reprinted from Electrochimica Acta, Volume 269, 10 April 2018, Pages 291–298.*

and the plasmon integrated semiconductor serves as an interesting system to fully understand how it manages energy flow via EM field enhancement and other physical and chemical processes at the nanometer scale. The theoretical modeling can predict the physical enhancement and requires well-defined geometry input and a high-reproducibility experimental approach to construct such a single-particle tip to compare with the theoretical prediction. The modeling geometry input needs an accurate consideration of the geometry and physical characteristics such as the refraction index variation introduced by the concentration gradient of local redox mediators, as well as the light absorption characteristics of the underlying semiconductor. The effect of local field enhancement on plasmonic NP held by an insulated tip, where the tip current is expected to be responsive to light absorption and light scattering of all components. It should be noted that the experimentally generated Au NPs are not ideally spherical, therefore a more advanced modeling tool is needed to model the optical properties of an irregular NP geometry. Improved theory prediction needs to adjust the electrode input geometry and reaction mechanism involved in a PEC reaction to compare theory and experimental results. Finally, other contributing factors such as enhanced catalytic and conductivity activities of plasmon nanostructures to the PEC performance of a photoelectrode need to be investigated.

Credit author statement

S.P. acquired funding, contributed to conceptualization, and performed writing, reviewing, and editing. M.A. and E.W. are currently performing a single nanoparticle electrode project and contributed to collecting/summarizing literature, and X.L. is currently working on plasmon-enhanced PEC. M.A., E.W., and X.L. performed reviewing and editing. M.A. performed writing on nanoelectrode fabrication.

Declaration of competing interest

The authors declare that they have no known competing financial interests or personal relationships that could have appeared to influence the work reported in this article.

Data availability

Data will be made available on request.

Acknowledgments

We acknowledge National Science Foundation for supporting this work under Award Number CBET-2113505. S.P. acknowledges the support of Marilyn Williams Elmore and John Durr Elmore Professor fellowship.

Appendix A. Supplementary data

Supplementary data to this article can be found online at https://doi.org/10.1016/j.coelec.2022.101174.

References

Papers of particular interest, published within the period of review, have been highlighted as:

* * of outstanding interest

1. Yu F, Persson B, Loefs S, Knoll W: *J Am Chem Soc* 2004, **126**: 8902–8903.

2. Xu F, Zhen G, Yu F, Kuennemann E, Textor M, Knoll W: *J Am Chem Soc* 2005, **127**:13084–13085.

3. Su X, Wu Y-J, Robelek R, Knoll W: *Langmuir* 2005, **21**:348–353.

4. ** Pan S, Li X, Yadav J: *Phys Chem Chem Phys* 2021, **23**: 19120–19129.
This is a most recent review written by the author on surface plasmon resonance for quantitative analysis and single particle spectroelectrochemistry analysis. This is among those few reviews based on the author's recent decade of research in this field. The key methods described in this work are the bases for the photocatalysis study described in this work.

5. Linic S, Christopher P, Ingram DB: *Nat Mater* 2011, **10**:911–921.

6. ** Strange LE, Yadav J, Li X, Pan S: *J Electrochem Soc* 2020, **167**, 146518.
This work published by the author's group uses electrodeposition to produce Transition metal dichalcogenides (TMD) and TMD bilayer electrodes using sequential electrodeposition for electrocatalytic hydrogen evolution reaction (HER). The results presented include cost-effective deposition techniques along with enhanced proton reduction activity for the sequentially deposited bilayer TMD structure consisting of MoS2 and MoSe2, which suggests the electron transfer kinetics from the conductive glass substrate to the top layer is enhanced with a MoS2 layer.

7. ** Shan Z, Clayton D, Pan S, Archana PS, Gupta A: *J Phys Chem B* 2014, **118**:14037–14046.
This work presents a model electrode system comprised of nanostructured Ti electrode sensitized with Ag@Ag_2S core–shell nanoparticles (NPs) for surface plasmon driven photoelectrochemistry studies. Pronounced photoelectrochemical responses of Ag@Ag_2S NPs under visible light were obtained and attributed to collective contributions of visible light sensitivity of Ag_2S, the local field enhancement of Ag surface plasmon, enhanced charge collection by Ti@TiO2 NWs, and the high surface area of the nanostructured electrode system.

8. ** Wang J, Pan S, Chen M, Dixon DA: *J Phys Chem C* 2013, **117**: 22060–22068.
Surface plasmon-enhanced light absorption for photoelectrochemical water splitting at α-Fe_2O_3 thin film electrode coated with Au nanorods (NRs) is described. The significant increase in photocurrent in the region of surface plasmon absorption is attributed to the enhanced visible light absorption of α-Fe_2O_3 in the presence of the plasmon active Au NRs.

9. ** Archana PS, Pachauri N, Shan Z, Pan S, Gupta A: *J Phys Chem C* 2015, **119**:15506–15516.
This article report the enhanced photoelectrochemical (PEC) performance of a hematite film embedded with Au nanoparticles (NPs). The plasmonic enhancement increases with the amount of Au NPs for the same thickness of hematite. Thickness-dependent study of photoactivity indicates a higher enhancement in hematite thin films compared to thicker films due to reduced charge transport distance and optimal local field enhancement effect.

10. Zhang X, Zhu Y, Yang X, Wang S, Shen J, Lin B, Li C: *Nanoscale* 2013, **5**:3359–3366.

11. Lee J, Mubeen S, Ji X, Stucky GD, Moskovits M: *Nano Lett* 2012, **12**:5014–5019.

12. Mubeen S, Lee J, Singh N, Kraemer S, Stucky GD, Moskovits M: *Nat Nanotechnol* 2013, **8**:247–251.

13. Zhang H, Wang G, Chen D, Lv X, Li J: *Chem Mater* 2008, **20**: 6543–6549.

14. Zheng J, Yu H, Li X, Zhang S: *Appl Surf Sci* 2008, **254**:1630–1635.

15. Gorzkowska-Sobas A, Kusior E, Radecka M, Zakrzewska K: *Surf Sci* 2006, **600**:3964–3970.

16. Sun L, Li J, Wang C, Li S, Lai Y, Chen H, Lin C: *J Hazard Mater* 2009, **171**:1045–1050.

17. He J, Yang P, Sato H, Umemura Y, Yamagishi A: *J Electroanal Chem* 2004, **566**:227–233.

18. Zhao G, Kozuka H, Yoko T: *Thin Solid Films* 1996, **277**:147–154.

19. Subramanian V, Wolf EE, Kamat PV: *J Am Chem Soc* 2004, **126**: 4943–4950.

20. Dubi Y, Un IW, Sivan Y: *Chem Sci* 2020, **11**:5017–5027.

21. Mascaretti L, Naldoni A: *J Appl Phys* 2020, **128**, 041101.

22. Bumajdad A, Madkour M: *Phys Chem Chem Phys* 2014, **16**: 7146–7158.

23. Thimsen E, Le Formal F, Gratzel M, Warren SC: *Nano Lett* 2011, **11**:35–43.

24. Gao H, Liu C, Jeong HE, Yang P: *ACS Nano* 2012, **6**:234–240.

25. Thomann I, Pinaud BA, Chen Z, Clemens BM, Jaramillo TF, Brongersma ML: *Nano Lett* 2011, **11**:3440–3446.

26. Ma Y, Shinde PS, Li X, Pan S: *ACS Omega* 2019, **4**: ** 17257–17268.
Au-modified hematite photoanode was screened for photoelectrochemical (PEC) water oxidation by the scanning electrochemical microscopy (SECM) technique with a scanning probe of the optical fiber for visible light irradiation of the photoanode substrate. The Au-modified hematite exhibited an enhancement in the photocurrent up to 3% (at. %), and the performance drop was observed with 4–10% (at. %) of Au modification.

27. Warren SC, Thimsen E: *Energy Environ Sci* 2012, **5**:5133–5146.

28. Pan S, Liu J, Hill CM: *J Phys Chem C* 2015, **119**:27095–27103. **
This publication shows that Electrogenerated Chemiluminescence (ECL) generation at individual Au NPs increases with particle size (diameters from 30 to 300 nm) and is affected by the local chemical and charge transfer environment of the NPs. Such an ECL detection scheme can allow one to study the local redox activities of single nanoparticles with improved spatial resolution. ECL at single Au NPs shows slight temporal variations in intensity attributed to the oxidation and reconstruction of small clusters on the Au surface during ECL generation.

29. Wusimanjiang Y, Ma Y, Lee M, Pan S: *Electrochim Acta* 2018, ** **269**:291–298.
The auhtors present the fabrication and spectroelectrochemistry characteristics of light-scattering single Au NP at the tip of an electrochemically etched sharp tungsten (W)electrode. Au NPs with a tunable particle size can be obtained at the W tips by adjusting the Au electrodeposition conditions. Catalyzed electrogenerated chemiluminescence (ECL) at a single Au NP electrode shows an increase in its intensity with Au NP particle size in the range of 300 nm–500 nm. This unique electrode configuration provides useful features for spectroelectrochemistry characterization at the nanometer scale.

30. Saqib M, Fan Y, Hao R, Zhang B: *Nano Energy* 2021:90.

31. Chen R, Hu K, Yu Y, Mirkin MV, Amemiya S: *J Electrochem Soc* ** 2016, **163**:H3032–H3037.
The authors developed unique carbon nanoprobes with high electrochemical reactivity and well-controlled size and geometry based on chemical vapor deposition of carbon in quartz nanopipets. Carbon-filled nanopipets are milled by focused ion beam (FIB) technology to yield flat disk tips with a thin quartz sheath as confirmed by transmission electron microscopy.

32. Mao G, Kilani M, Ahmed M: *J Electrochem Soc* 2022:169.

33. Nellist MR, Chen Y, Mark A, Godrich S, Stelling C, Jiang J, Poddar R, Li C, Kumar R, Papastavrou G, Retsch M, Brunschwig BS, Huang Z, Xiang C, Boettcher SW: *Nanotechnology* 2017, **28**, 095711.

34. Zhang Y, Xu S, Qian Y, Yang X, Li Y: *RSC Adv* 2015, **5**: 77248–77254.

35. Noël J-M, Velmurugan J, Gökmeşe E, Mirkin MV: *J Solid State* ** *Electrochem* 2012, **17**:385–389.
This work developed a method for controlled chemical etching of silver in ammonia solutions to produce recessed nanoelectrodes. Voltammograms and SECM approach curves were obtained to evaluate the recess depth and other geometric parameters of the etched electrodes.

36. Li H-N, Yang D, Liu A-X, Liu G-H, Shan Y-P, Yang G-C, He J: *Chin J Anal Chem* 2019, **47**:e19104–e19112.

37. Zhu X, Qiao Y, Zhang X, Zhang S, Yin X, Gu J, Chen Y, Zhu Z, Li M, Shao Y: *Anal Chem* 2014, **86**:7001–7008.

38. Yu Y, Noel JM, Mirkin MV, Gao Y, Mashtalir O, Friedman G, ** Gogotsi Y: *Anal Chem* 2014, **86**:3365–3372.
This publication demonstrated the possibility of using nanometer-sized quartz pipettes with a layer of carbon deposited on the inner wall for sampling attoliter-to-picoliter volumes of fluids and determining redox species by voltammetry and coulometry. Very fast mass-transport inside the carbon-coated nanocavity allows for rapid exhaustive electrolysis of the sampled material.

39. Takahashi Y, Shevchuk AI, Novak P, Babakinejad B, Macpherson J, Unwin PR, Shiku H, Gorelik J, Klenerman D, Korchev YE, Matsue T: *Proc Natl Acad Sci U S A* 2012, **109**: 11540–11545.